

Phosphorus Ligands

International Edition: DOI: 10.1002/anie.201601775
German Edition: DOI: 10.1002/ange.201601775Unexpected Reactivity of $[(\eta^5\text{-}1,2,4\text{-}t\text{Bu}_3\text{C}_5\text{H}_2)\text{Ni}(\eta^3\text{-P}_3)]$ towards Main Group Nucleophiles and by Reduction

Eric Mädl, Gábor Balázs, Eugenia V. Peresyphina, and Manfred Scheer*

Dedicated to Professor Peter Klüfers on the occasion of his 65th birthday

Abstract: The reduction of $[\text{Cp}'''\text{Ni}(\eta^3\text{-P}_3)]$ (**1**; $\text{Cp}''' = \eta^5\text{-}1,2,4\text{-}t\text{Bu}_3\text{C}_5\text{H}_2$) with potassium produces the complex anion $[(\text{Cp}'''\text{Ni})_2(\mu, \eta^{2:2}\text{-P}_8)]^{2-}$ (**2**), which contains a realgar-like P_8 unit. The anionic triple-decker sandwich complex $[(\text{Cp}'''\text{Ni})_2(\mu, \eta^{3:3}\text{-P}_3)]^-$ (**3**) with a cyclo- P_3 middle deck is obtained when **1** is treated with NaNH_2 as a nucleophile. **Na[3]** can subsequently be oxidized with AgOTf to the neutral triple-decker complex $[(\text{Cp}'''\text{Ni})_2(\mu, \eta^{3:3}\text{-P}_3)]$ (**4**). In contrast, **1** reacts with LiPPh_2 to give the anionic compound $[(\text{Cp}'''\text{Ni})_2(\mu, \eta^{2:2}\text{-P}_6\text{PPh}_2)]^-$ (**5**), a complex containing a bicyclic P_7 fragment capped by two $\text{Cp}'''\text{Ni}$ units. Protonation of **Li[5]** with HBF_4 leads to the neutral complex $[(\text{Cp}'''\text{Ni})_2(\mu, \eta^{2:2}\text{-(HP}_6\text{PPh}_2)]$ (**6**). Adding LiNMe_2 to **1** results in $[\text{Cp}'''\text{Ni}(\eta^2\text{-P}_3\text{NMe}_2)]^-$ (**7**) becoming accessible, a complex which forms as a result of nucleophilic attack at the cyclo- P_3 ring of **1**. The complexes **K₂[2]**, **Na[3]**, **4**, **6**, and **Li[7]** were fully characterized and their structures determined by single-crystal X-ray diffraction.

The stoichiometric and catalytic reactivity of organometallic compounds is one of the most active research topics in chemistry. The methine unit $-\text{CH}-$ is related through an isolobal relationship to a naked P atom. Therefore, mixed P- and CR-containing complexes have attracted considerable attention,^[1] and novel approaches to phosphorus- and arsenic-rich aromatic starting materials^[2] have opened new avenues for the fine-tuning of such mixed complexes. Compared to the isolobal CH fragments, the stereochemically active lone pairs of electrons on the ring P atoms are additionally able to coordinate to Lewis-acidic moieties, thereby turning them into valuable starting materials in coordination chemistry^[3] and catalysis.^[4] In this respect, the all-phosphorus or all-arsenic analogues of such ligands are of unique interest in organometallic complexes since they can form unprecedented

coordination polymers,^[5] which can themselves function as molecular capsules for the stabilization of otherwise unstable or unknown molecules.^[6] However, giant molecular nanoclusters with fullerene-like topology can be formed by employing fivefold symmetry, such as, for example, in the case of pentaphosphaferrocene $[\text{Cp}^*\text{Fe}(\eta^5\text{-P}_5)]$.^[7]

Recently, the redox behavior of $[\text{Cp}^*\text{Fe}(\eta^5\text{-P}_5)]$ was investigated, which led to the dianionic complexes $[\text{Cp}^*\text{Fe}(\eta^4\text{-P}_5)]^{2-}$ and $[(\text{Cp}^*\text{Fe})_2(\mu, \eta^{4:4}\text{-P}_{10})]^{2-}$, as well as to the dicationic compound $[(\text{Cp}^*\text{Fe})_2(\eta^{5:5}\text{-P}_{10})]^{2+}$.^[8] This electrochemical behavior is in contrast to the reactivity of the phosphorus-free compound ferrocene.^[9] Moreover, the reaction of main group nucleophiles with pentaphosphaferrocene could lead a new direction of reactivity being found and, thus, versatile functionalization and unexpected connectivity patterns could be realized.^[10] The nucleophiles add on the cyclo- P_5 ligand, thereby leading to an envelope conformation of the ring. The use of organic nucleophiles leads to P–C bonds being formed, which is a first step in the transformation to organophosphorus ligands. The question arises whether this reactivity is limited to pentaphosphaferrocene or, if extendable, what the scope and perspectives will be.

$[\text{Cp}'''\text{Ni}(\eta^3\text{-P}_3)]$ (**1**; $\text{Cp}''' = \eta^5\text{-}1,2,4\text{-}t\text{Bu}_3\text{C}_5\text{H}_2$) seems to be a promising starting material to investigate these topics. DFT calculations suggest a high reactivity towards main group nucleophiles or reducing agents. The HOMO of **1** does not reflect any donor properties of the P atom (Figure 1), which is in line with our unsuccessful attempts to use this compound for supramolecular aggregation. The LUMO, however, is located on the cyclo- P_3 unit, similar to the pentaphosphaferrocene $[\text{Cp}^*\text{Fe}(\eta^5\text{-P}_5)]$,^[11] which indicates that a reduction or a nucleophilic attack should occur at the phosphorus ring.

Herein we report on the reduction of **1** to give, for the first time, a complete structural rearrangement and reaggregation

[*] Dr. E. Mädl, Dr. G. Balázs, Prof. Dr. M. Scheer
Institut für Anorganische Chemie, Universität Regensburg
93051 Regensburg (Germany)
E-mail: Manfred.scheer@ur.de
Homepage: <http://www.ur.de/chemie-pharmazie/anorganische-chemie-scheer/>

Dr. E. V. Peresyphina
Nikolaev Institute of Inorganic Chemistry
Siberian Division of RAS
Acad. Lavrentyev str. 3, 630090 Novosibirsk (Russia)
and
Novosibirsk State University
Pirogova str. 2, 630090 Novosibirsk (Russia)

Supporting information for this article can be found under:
<http://dx.doi.org/10.1002/anie.201601775>.

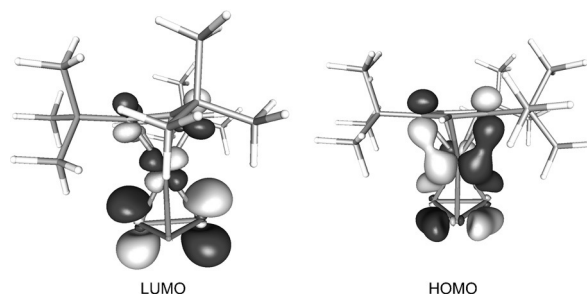
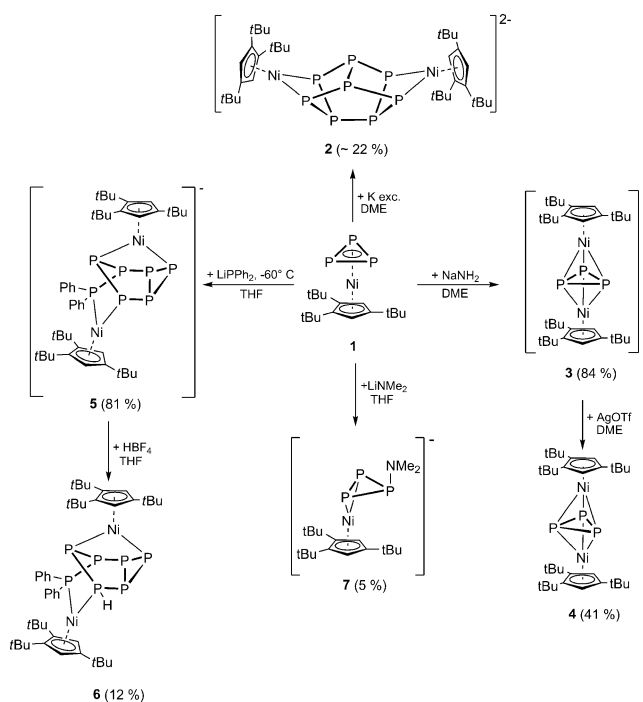


Figure 1. Selected molecular orbitals of **1** calculated at the BP86/def2-TZVP level of theory.

of a *cyclo*- P_n ligand complex, with formation of an unprecedented dianionic dinuclear complex with a P_8 realgar-type structural moiety. Furthermore, the reaction with nucleophiles leads to a structural rearrangement to form either an anionic triple-decker sandwich complex, or—with $[PPh_2]^-$ as the nucleophile—after addition, a ring expansion is observed to give a novel P_7Ph_2 ligand which is coordinated by two $Cp''Ni$ moieties (Scheme 1). These unexpected results show the potential of complex **1** to act as a phosphorus-based building block with diverse structural reorganizations.



Scheme 1. Reactivity of **1** towards different nucleophiles and potassium as well as subsequent reactions. If not stated differently, the reactions were carried out at room temperature.

The reduction of **1** by potassium leads to formation of $K_2[2]$, along with the triple-decker complex $K[3]$ in a ratio of 1:5. The C_{2v} symmetry of $K_2[2]$ results in an $AA'MM'XX'X''$ spin system in the ^{31}P NMR spectrum, with multiplets centered at 30.6, 10.1, and -17.9 ppm. The assignment of the AA' and MM' signals was achieved by simulation of the ^{31}P NMR spectrum.^[12] Single crystals suitable for X-ray structural analysis were obtained by adding 18-crown-6 to a solution of $K_2[2]$ in DME. The molecular structure of $[K_2(18-c-6)_2(DME)][2]$ shows a P_8 realgar-like core coordinating to two 15 valence electron (VE) $Cp''Ni$ fragments (Figure 2). Although there are a few known complexes containing a P_8 structural motif, this is the first ionic compound with such a polyphosphorus cage.^[13] All the bond lengths in the P_8 core are in the range of P–P single bonds (2.191(3)–2.243(4) Å) and are similar to the corresponding bond lengths in other related P_8 derivatives. The formation of **2** shows that the reaction with strong reducing agents enables **1** to act as a phosphorus source and thereby

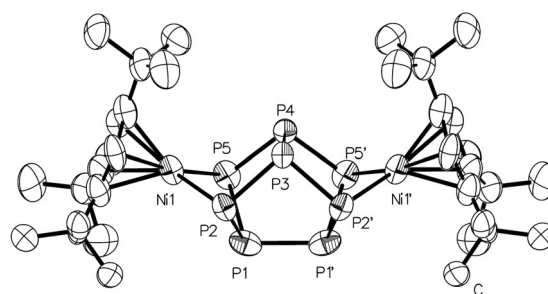


Figure 2. Molecular structure of the anionic part of $[K_2(18-c-6)_2(DME)][2]$. H atoms bonded to carbon are omitted for clarity. Ellipsoids are drawn at the 50% probability level. Selected bond lengths [Å] and angles [°]: P1–P2 2.191(3), P1–P5 2.206(3), P1–P1' 2.243(4), P2–P3 2.200(2), P3–P4 2.212(3), P4–P5 2.210(2), P4–P5 2.211(2), Ni1–P2 2.211(2), Ni1–P5 2.216(2); P2–P1–P5 84.87(9), P2–P1–P1' 103.93(7), P5–P1–P1' 104.35(8), P1–P2–P3 98.46(10), P1–P2–Ni1 85.26(9), P3–P2–Ni1 102.70(9), P2–P3–P2' 97.12(14), P2–P3–P4 100.09(10), P5–P4–P5' 98.02(15), P5–P4–P3 99.64(10), P1–P5–P4 98.06(10), P1–P5–Ni1 84.76(9), P4–P5–Ni1 102.77(10).

lead after rearrangement to larger phosphorus aggregates. Natural population analysis (NPA) on **2** shows that the phosphorus atoms, which coordinate to Ni atoms are negatively charged (-0.26), while the Ni centers bear a positive charge of $+0.45$. The noncoordinating phosphorus atoms are only slightly negatively charged (-0.14 , -0.15).

The reduction of **1** to **2** is accompanied by the formation of the triple-decker complex **3**, and it was not possible to separate both in an analytically pure manner. However, we found that adding $NaNH_2$ to **1** appears to be a straightforward method to synthesize the triple-decker complex $Na[3]$ in 84 % yield (Scheme 1). In contrast, the reaction of pentaphosphaferrocene with $NaNH_2$ leads to a nucleophilic attack and a subsequent autometalation to afford the trianionic moiety $[(Cp^*Fe(\eta^4-P_5))_2N]^{3-}$.^[10] Compound $Na[3]$ was characterized by multinuclear NMR spectroscopy in $[D_8]THF$, with a singlet observed in the ^{31}P NMR spectrum at -346.5 ppm, which is shifted strongly to higher field compared to that of **1** (-163.4 ppm) and is close to the chemical shift of the neutral compound $[Cp''Mo(CO)_2(\eta^3-P_3)]$ (-348.9 ppm).^[14] Cyclic voltammetric studies of **3** in acetonitrile show one reversible oxidation with a half-potential of -1.46 V.^[15] In addition, an irreversible reduction at -2.13 V is observed. No further oxidations or reductions at higher or lower potentials occur. On the basis of these results, an equimolar solution of $AgOTf$ in DME was added to a solution of **3** in DME, which led to a color change to yellow-green and the immediate formation of a silver mirror. After purification by column chromatography, the neutral triple-decker complex $[(Cp''Ni)_2(\eta^{3.3}-P_3)]$ (**4**) was isolated in 41 % yield (Scheme 1). The 33 valence electron complex **4** was characterized by EPR spectroscopy and the magnetic moment was determined by the Evans method.^[12] The effective magnetic moment of $\mu_{eff} = 1.92 \mu_B$ corresponds to one unpaired electron. DFT calculations on **4** reveal that the spin density is mainly localized on the two Ni atoms, with minor contributions on the *cyclo*- P_3 phosphorus atoms and the Cp ligands.

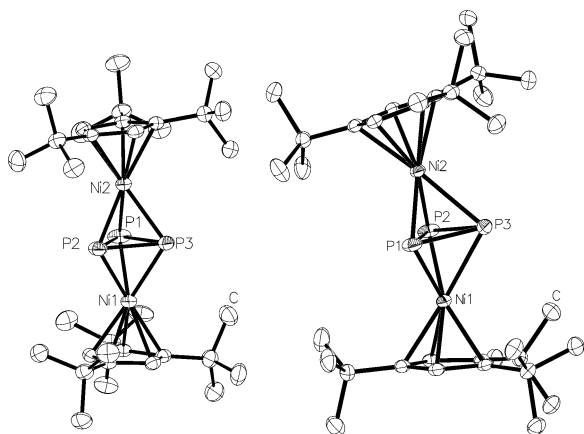


Figure 3. Molecular structure of the anionic part of $[\text{Na}(\text{dme})_4][\mathbf{3}]$ (left) and the neutral compound **4** (right). H atoms bonded to carbon are omitted for clarity. Ellipsoids are drawn at the 50% probability level. Selected bond lengths [Å] and angles [°]: $[\text{Na}(\text{dme})_4][\mathbf{3}]$: P1–P2: 2.2408(7), P1–P3: 2.1950(7), P2–P3: 2.2094(6), Ni1–P1: 2.2621(5), Ni1–P2: 2.2508(5), Ni1–P3: 2.2807(5); P2–P1–P3: 59.74(2), P1–P2–P3: 59.10(2), P1–P3–P2: 61.16(2). **4**: P1–P2: 2.3976(6), P1–P3: 2.1851(6), P2–P3: 2.1817(5), Ni1–P1: 2.2077(4), Ni1–P2: 2.2086(4), Ni1–P3: 2.3778(4); P2–P1–P3: 56.63(2), P1–P2–P3: 56.77(2), P1–P3–P2: 66.60(2).

X-ray structural analysis of $[\text{Na}(\text{dme})_4][\mathbf{3}]$ and **4** show sandwich triple-decker complexes with a three-membered phosphorus ring as a middle deck: anionic for **3** and neutral for **4** (Figure 3). In contrast to anion **3**, in which the P–P single bonds result in a nondistorted P_3 ring (P–P bonds: 2.1950(7)–2.2408(7) Å), in **4** two P–P bond lengths are shortened (P1–P2: 2.1851(6) Å; P2–P3: 2.1817(5) Å) and one is elongated (P1–P3: 2.3976(6) Å), which reveals, therefore, an allylic distortion. The three-membered ring in **3** is symmetrically coordinated in a $\eta^{3:3}$ fashion to both nickel atoms (P–Ni1: 2.2508(5)–2.2807(5) Å; P–Ni2: 2.2519(5)–2.2875(5) Å). A similar structural motif was reported for the dicationic compound $[\text{Ni}(\text{CH}_3\text{C}(\text{CH}_2\text{PPh}_2)_3)_2](\mu, \eta^{3:3}\text{-P}_3)[\text{BPh}_4]_2$.^[16] The Ni–P bonds differ in **4** (P1–Ni1: 2.2077(4) Å, P2–Ni1: 2.2086(4) Å, P3–Ni1: 2.3778(4) Å) and, as a result, the P_3 ring is shifted out of the center of the complex, thereby resulting in a nonlinear conformation (Ni1–P_{3center}–Ni2: 176.89(1)° in **3**; Ni1–P_{3center}–Ni2: 160.67(1)° in **4**).

DFT calculations on the model compounds $[(\text{CpNi})_2(\mu, \eta^{3:3}\text{-P}_3)]^{+/0/-}$ (Figure 4) show that the distortion of the P_3 unit from the allylic to the symmetrical *cyclo*- P_3 unit is caused by the stepwise population of a P–P bonding molecular orbital, on going from the cation $[(\text{CpNi})_2(\mu, \eta^{3:3}\text{-P}_3)]^+$ to the anion $[(\text{CpNi})_2(\mu, \eta^{3:3}\text{-P}_3)]^-$. This MO represents the lowest unoccupied orbital (LUMO) in $[(\text{CpNi})_2(\mu, \eta^{3:3}\text{-P}_3)]^+$ and the highest occupied MO (HOMO) in the anion $[(\text{CpNi})_2(\mu, \eta^{3:3}\text{-P}_3)]^-$. The increase in the strength of the P–P bond on going from $[(\text{CpNi})_2(\mu, \eta^{3:3}\text{-P}_3)]^+$ to $[(\text{CpNi})_2(\mu, \eta^{3:3}\text{-P}_3)]^-$ is confirmed by the Wiberg bond index (WBI), which varies from 0.35 over 0.69 to 0.94.

Regardless of several attempts, no further information concerning the pathway of the reaction of **1** with NaNH_2 to form **3** (Scheme 1) could be obtained. No insoluble polyphosphorus compounds are formed, and no soluble phospho-

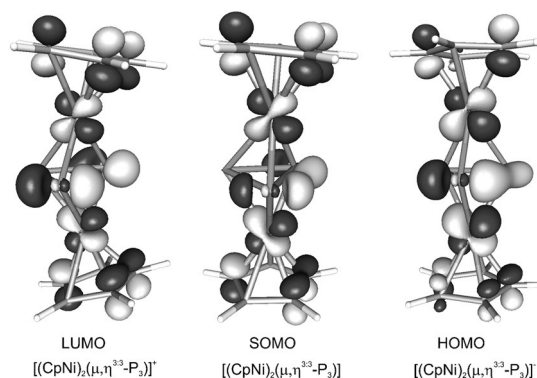


Figure 4. Frontier molecular orbitals for $[(\text{CpNi})_2(\mu, \eta^{3:3}\text{-P}_3)]^{+/0/-}$, calculated at the BP86/def2-TZVP level of theory.

rus-containing by-products could be detected in the ^{31}P NMR spectrum.^[17] To our knowledge, complexes **3** and **4** are the first anionic and neutral nickel–nickel triple-decker sandwich complexes exhibiting a $\eta^{3:3}\text{-P}_3$ middle deck with cyclopentadienyl ligands.^[16,18]

Treatment of **1** with LiPPh_2 at room temperature leads to the formation of $[\text{Li}][(\text{Cp}''\text{Ni})_2(\mu, \eta^{2:2}\text{-P}_6\text{PPh}_2)]^-$ (**Li[5]**; Scheme 1). The ^{31}P NMR spectrum of the crude reaction mixture shows seven multiplets, centered at 212.1, 135.8, 106.7, 74.0, –48.50, –119.6, and –133.8 ppm, which can be attributed to **5**, as proven by a ^{31}P , ^{31}P -COSY experiment.^[12,19] Additionally, two unassigned signals at 7.4 and –14.2 ppm were observed. All the coupling constants obtained from the simulation of the ^{31}P NMR spectrum of **5** lie in the expected range.^[12] All attempts to crystallize and purify **5** failed because of its high sensitivity. Therefore, **5** was treated with an equimolar amount of HBF_4 to give the protonated species $[(\text{Cp}''\text{Ni})_2(\mu, \eta^{2:2}\text{-HP}_6\text{PPh}_2)]$ (**6**), which could be isolated after column chromatographic work up. The ^{31}P NMR spectrum of **6** shows seven multiplets centered at 140.2, 105.0, 35.4, –35.15, –132.5, and –211.05 ppm.^[12] Single crystals suitable for X-ray diffraction measurements were obtained from a pentane solution. The molecular structure of **6** reveals a bicyclic P_6 ligand containing an exocyclic PPh_2 unit, which coordinates to two $\text{Cp}''\text{Ni}$ fragments (Figure 5). The position of the hydrogen atom bonded to the P2 atom could be localized from the difference electron density map and was also proven by ^{31}P NMR spectroscopy in solution. All the P–P bonds are in the range of single bonds (2.1778(9)–2.2241(8) Å). The NPA of **6** shows a positive charge concentration on the Ni and P7 atoms (Ni1: 0.46, Ni2: 0.49, and P7: 0.69); the P1 and P4 atoms bear negative charges (–0.20 and –0.13, respectively). The other phosphorus atoms are essentially neutral.

A reaction pathway for the formation of the P_7 ligand in **5** involving intermediate **A** is proposed (Scheme 2). To gain further insight, an excess of three equivalents of LiPPh_2 was added to **1**, to prevent the subsequent reaction of **A** with another equivalent of **1**. The ^{31}P NMR spectrum of this reaction mixture at 193 K shows three signals centered at 16.3 (dt, $^1J_{\text{P-P}} = 291.7$ Hz; $^2J_{\text{P-P}} = 54.5$ Hz), –142.6 (dd, $^1J_{\text{P-P}} = 195.7$, $^2J_{\text{P-P}} = 54.5$), and –187.3 (dt, $^1J_{\text{P-P}} = 291.7$, $^1J_{\text{P-P}} = 196.8$ Hz)

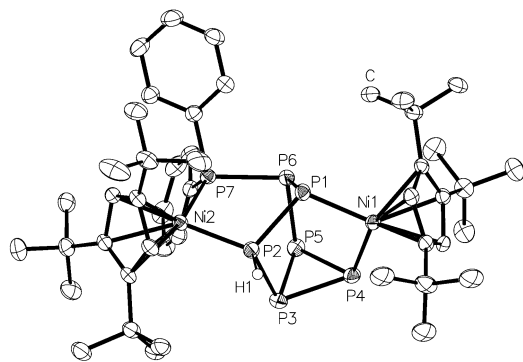
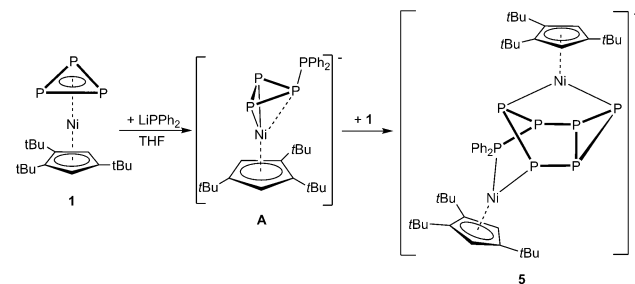


Figure 5. Molecular structure of **6**-C₅H₁₂. H atoms bonded to carbon and the solvated pentane molecules are omitted for clarity. Ellipsoids are drawn at the 50% probability level. Selected bond lengths [Å] and angles [°]: P1–Ni1 2.1711(5), P1–P2 2.1789(6), P1–P6 2.1840(6), P2–Ni2 2.1663(5), P2–P3 2.2003(6), P2–H1 1.26(2), P3–P4 2.2012(6), P3–P5 2.2154(6), P4–Ni1 2.1864(5), P4–P5 2.2199(6), P5–P6 2.2241(6), P6–P7 2.2244(6), P7–Ni2 2.1759(5); P2–P1–P6 88.61(2), P1–P2–P3 105.67(2), P2–P3–P4 100.28(2), P2–P3–P5 96.44(2), P4–P3–P5 60.348(19), P3–P4–P5 60.14(2), P3–P5–P4 59.51(2), P3–P5–P6 104.78(2), P4–P5–P6 96.99(2), P1–P6–P5 103.94(2), P1–P6–P7 98.36(2), P5–P6–P7 99.42(2).



Scheme 2. Proposed reaction pathway for the formation of **5**.

ppm, which confirms the structure of intermediate **A**. Furthermore, two unassigned signals centered at -139.8 (d, $^1J_{\text{P-P}} = 197.2$) and -171.5 (t, $^1J_{\text{P-P}} = 197.2$) were recorded, in addition to one sharp singlet at -21.5 ppm for LiPPh₂. Warming the sample up to room temperature resulted in the signals for **A** decreasing in intensity and finally disappearing. Concomitantly, the signal for LiPPh₂ broadened and a very broad signal at -158.9 ppm became visible, which is very similar to the ^{31}P chemical shift of the starting material **1** (-163.4 ppm).^[12,20] This broad signal, together with the previous observations, can be explained by a fluxional process of **A** in solution. This is also in line with the corresponding DFT calculations. According to these, **A** possesses elongated P–PPh₂ (2.367 Å) as well as Ni–P(PPh₂) (2.804 Å) bonds, with Wiberg bond orders (WBI) of 0.81 and 0.28, respectively. The WBIs of the other two Ni–P bonds are 0.81 and 0.79. The reaction of **1** with LiPPh₂ to **A** is favored by -39.2 kJ mol⁻¹ in solution, whereas the reaction of **A** with **1** is slightly more exothermic (-45.0 kJ mol⁻¹; Figure 6). The weakening of one Ni–P bond leads to an increased reactivity of **A** towards **1**, thereby giving, after rearrangement, the bicyclic complex **5**.^[21]

To the best of our knowledge, there is no other example of a bicyclic phosphorus ligand such as that found in **5** that

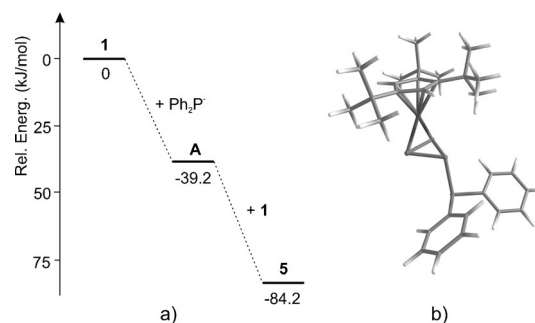


Figure 6. a) Energy profile of the reaction of **1** with Ph₂P⁻ and b) optimized geometry of **A**, calculated at the BP86/def2-TZVP level of theory.

coordinates to a transition metal. However, the organic-substituted, neutral, and uncoordinated 2,3,4,6-tetra-*tert*-butylbicyclo[3.1.0]hexaphosphane is known^[22] and the compound [P₇Cy₆][OTf] was synthesized recently.^[23]

The formation of the sandwich triple-decker complex **3** cannot be observed if LiNMe₂ (not NaNH₂, as used above) is treated with **1** in THF.^[24] Instead, the addition of 1.5 equivalents of LiNMe₂ results in the ^{31}P NMR spectrum showing the formation of two products in a ratio of 1:5. The minor product exhibits six multiplets centered at 180.1, 162.0, 65.3, 10.5, -109.9 , and -117.4 ppm with an integral ratio of 1:1:1:1:1:1, thus indicating the formation of a bicyclic analogue of **5**, which could not be isolated. The main product, [Cp''Ni(η²-P₃NMe₂)]⁻ (**7**), shows one triplet at -104.6 ppm ($^1J_{\text{P-P}} = 246.9$ Hz) and one doublet at -168.0 ppm ($^1J_{\text{P-P}} = 247.1$ Hz). This finding is in contrast to the reaction of **1** with LiPPh₂, which leads to the bicyclic species **5** as the main product, but confirms the first reaction product **A** (Scheme 2). A few crystals of [Li(thf)₃][**7**] were obtained by layering the solution with *n*-hexane. The X-ray structure analysis reveals a structural motif similar to **A** (Figure 7). The *cyclo*-P₃ ligand

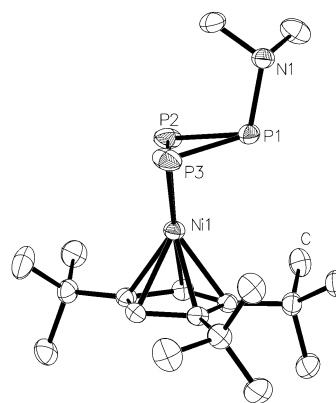


Figure 7. Molecular structure of the anionic part of [Li(thf)₃][**7**]. H atoms bonded to carbon are omitted for clarity. Ellipsoids are drawn at the 50% probability level. Selected bond lengths [Å] and angles [°]: P1–P2 2.1940(5), P1–P3 2.1736(6), P2–P3 2.1337(7), P1–Ni1 1.8196(13), Ni1–P2 2.2049(5), Ni1–P3 2.1979(5); P1–P2–P3 60.28(2), P1–P3–P2 61.24(2), P2–P1–P3 58.48(2).

in **7** coordinates in a η^2 fashion, and the noncoordinating phosphorus atom bears the NMe_2 unit. The P–P bond between the coordinating P atoms is shortened compared to the remaining P–P bonds (P–P bond lengths: 2.1337(7), 2.1736(6), 2.1940(5) Å). If a two equivalent excess of LiNMe_2 is used, **7** is formed exclusively, as proven by ^{31}P NMR spectroscopy. However, **7** decomposes during the work-up process because of its high sensitivity.

In summary, we have shown for the first time that the reduction of $[\text{Cp}''\text{Ni}(\eta^3\text{-P}_3)]$ (**1**) by potassium leads to reaggregation of P_n ligand complexes, with formation of the unprecedented complex anion $[(\text{Cp}''\text{Ni})_2(\mu, \eta^{2,2}\text{-P}_8)]^{2-}$ (**2**), which contains a realgar-like P_8 core. Furthermore, the reaction of **1** with NaNH_2 does not lead to substituted *cyclo*- P_3 compounds, but the anionic triple-decker complex $[(\text{Cp}''\text{Ni})_2(\mu, \eta^{3,3}\text{-P}_3)]^-$ (**3**) is formed instead. $\text{Na}[\textbf{3}]$ can be oxidized to its neutral derivative **4**, which contains a distorted P_3 middle deck. The reaction of Ph_2P^- as a nucleophile with **1** leads to a nucleophilic addition. However, the product **A** reacts further with **1** to form $[(\text{Cp}''\text{Ni})_2(\mu, \eta^{2,2}\text{-P}_6\text{PPh}_2)]^-$ (**5**), which can be trapped by protonation with HBF_4 to yield $[(\text{Cp}''\text{Ni})_2(\mu, \eta^{2,2}\text{-P}_6\text{HPPH}_2)]$ (**6**). The substituted compound $[\text{Cp}''\text{Ni}(\eta^2\text{-P}_3\text{NMe}_2)]^-$ (**7**) could be synthesized by changing the nucleophile to LiNMe_2 , which confirms the first found product $[\text{Cp}''\text{Ni}(\eta^2\text{-P}_3\text{PPh}_2)]^-$ (**A**) in the reaction leading to the formation of **5**.

Moreover, not only were we able to synthesize and characterize the aforementioned products, we have also found that **1** may serve as a readily accessible phosphorus source by separating the P_3 unit from its $\text{Cp}''\text{Ni}$ fragment. This observation has considerable potential to be investigated further.

Acknowledgments

We thank the Deutsche Forschungsgemeinschaft (DFG) for financial support and Dr. I. G. Shenderovich for the measurement of ^1H HSQC NMR spectra.

Keywords: electrophilic reactivity · nickel · phosphorus · reduction chemistry · triple decker complexes

How to cite: *Angew. Chem. Int. Ed.* **2016**, *55*, 7702–7707
Angew. Chem. **2016**, *128*, 7833–7838

- [1] a) J. F. Nixon, *Chem. Rev.* **1988**, *88*, 1327–1362; b) J. F. Nixon, *Coord. Chem. Rev.* **1995**, *145*, 201–258.
- [2] a) C. Heindl, E. V. Peresyphkina, A. V. Virovets, G. Balázs, M. Scheer, *Chem. Eur. J.* **2016**, *22*, 1944–1948; b) R. S. P. Turbervill, J. M. Goicoechea, *Chem. Rev.* **2014**, *114*, 10807–10828; c) R. S. P. Turbervill, J. M. Goicoechea, *Chem. Commun.* **2012**, 48, 6100–6102; d) A. S. Ionkin, W. J. Marshall, B. M. Fish, A. A. Marchione, L. A. Howe, F. Davidson, C. N. McEwen, *Eur. J. Inorg. Chem.* **2008**, 2386–2390.
- [3] a) M. Scheer, E. Herrmann, *Z. Chem.* **1990**, *29*, 41; b) O. J. Scherer, *Angew. Chem. Int. Ed. Engl.* **1990**, *29*, 1104; *Angew. Chem.* **1990**, *102*, 1137.
- [4] a) B. Breit, R. Winde, T. Mackewitz, R. Paciello, K. Harms, *Chem. Eur. J.* **2001**, *7*, 3106–3121; b) L. E. E. Broeckx, A. Bucci, C. Zuccaccia, M. Lutz, A. Macchioni, C. Müller, *Organometallics* **2015**, *34*, 2943–2952.
- [5] a) B. Attenberger, E. V. Peresyphkina, M. Scheer, *Inorg. Chem.* **2015**, *54*, 7021–7029; b) J. Bai, A. V. Virovets, M. Scheer, *Angew. Chem. Int. Ed.* **2002**, *41*, 1737–1740; *Angew. Chem.* **2002**, *114*, 1808–1811; c) M. Scheer, L. J. Gregoriades, A. V. Virovets, W. Kunz, R. Neueder, I. Krossing, *Angew. Chem. Int. Ed.* **2006**, *45*, 5689–5693; *Angew. Chem.* **2006**, *118*, 5818–5822; d) F. Dielmann, A. Schindler, S. Scheuermayer, J. Bai, R. Merkle, M. Zabel, A. V. Virovets, E. V. Peresyphkina, G. Brunklaus, H. Eckert, M. Scheer, *Chem. Eur. J.* **2012**, *18*, 1168–1179.
- [6] C. Schwarzmaier, A. Schindler, C. Heindl, S. Scheuermayer, E. V. Peresyphkina, A. V. Virovets, M. Neumeier, R. Gschwind, M. Scheer, *Angew. Chem. Int. Ed.* **2013**, *52*, 10896–10899; *Angew. Chem.* **2013**, *125*, 11097–11100.
- [7] a) J. Bai, A. V. Virovets, M. Scheer, *Science* **2003**, *300*, 781–783; b) M. Scheer, A. Schindler, J. Bai, B. P. Johnson, R. Merkle, R. Winter, A. V. Virovets, E. V. Peresyphkina, V. A. Blatov, M. Sierka, H. Eckert, *Chem. Eur. J.* **2010**, *16*, 2092–2107; c) M. Scheer, J. Bai, B. P. Johnson, R. Merkle, A. V. Virovets, C. E. Anson, *Eur. J. Inorg. Chem.* **2005**, 4023–4026; d) M. Scheer, A. Schindler, C. Gröger, A. V. Virovets, E. V. Peresyphkina, *Angew. Chem. Int. Ed.* **2009**, *48*, 5046–5049; *Angew. Chem.* **2009**, *121*, 5148–5151; e) M. Scheer, A. Schindler, R. Merkle, B. P. Johnson, M. Linseis, R. Winter, C. E. Anson, A. V. Virovets, *J. Am. Chem. Soc.* **2007**, *129*, 13386–13387; f) S. Welsch, C. Gröger, M. Sierka, M. Scheer, *Angew. Chem. Int. Ed.* **2011**, *50*, 1435–1438; *Angew. Chem.* **2011**, *123*, 1471–1474.
- [8] a) R. F. Winter, W. E. Geiger, *Organometallics* **1999**, *18*, 1827–1833; b) M. V. Butovskiy, G. Balázs, M. Bodensteiner, E. V. Peresyphkina, A. V. Virovets, J. Sutter, M. Scheer, *Angew. Chem. Int. Ed.* **2013**, *52*, 2972–2976; *Angew. Chem.* **2013**, *125*, 3045–3049.
- [9] a) M. D. Rausch, D. J. Ciappenelli, *J. Organomet. Chem.* **1967**, *10*, 127; b) A. G. Osborne, R. H. Whiteley, *J. Organomet. Chem.* **1978**, *162*, 79–81; c) M. Rausch, M. Vogel, H. Rosenberg, *J. Org. Chem.* **1957**, *22*, 903–906.
- [10] E. Mädl, M. V. Butovskii, G. Balázs, E. V. Peresyphkina, A. V. Virovets, M. Seidl, M. Scheer, *Angew. Chem. Int. Ed.* **2014**, *53*, 7643–7646; *Angew. Chem.* **2014**, *126*, 7774–7777.
- [11] a) H. Krauss, G. Balázs, M. Bodensteiner, M. Scheer, *Chem. Sci.* **2010**, *1*, 337–342; b) E. J. P. Malar, *Eur. J. Inorg. Chem.* **2004**, 2723–2732.
- [12] See the Supporting Information.
- [13] a) M. E. Barr, B. R. Adams, R. R. Weller, L. F. Dahl, *J. Am. Chem. Soc.* **1991**, *113*, 3052–3060; b) S. N. Konchenko, N. A. Pushkarevsky, M. T. Gamer, R. Köppe, H. Schnöckel, P. W. Roesky, *J. Am. Chem. Soc.* **2009**, *131*, 5740–5741; c) C. P. Butts, M. Green, T. N. Hooper, R. J. Kilby, J. E. McGrady, D. A. Pantazis, C. A. Russell, *Chem. Commun.* **2008**, 856–858; d) M. Scheer, U. Becker, E. Matern, *Chem. Ber.* **1996**, *129*, 721–724; e) W. Huang, P. L. Diaconescu, *Chem. Commun.* **2012**, 48, 2216–2218; f) F. Spitzer, C. Graßl, G. Balázs, E. M. Zolnhofer, K. Meyer, M. Scheer, *Angew. Chem. Int. Ed.* **2016**, *55*, 4340–4344.
- [14] M. Scheer, G. Friedrich, K. Schuster, *Angew. Chem. Int. Ed. Engl.* **1993**, *32*, 593–594; *Angew. Chem.* **1993**, *105*, 641–643.
- [15] Referenced against ferrocene.
- [16] M. Di Vaira, S. Midollini, L. Sacconi, *J. Am. Chem. Soc.* **1979**, *101*, 1757–1763.
- [17] Only traces of **[2]** are observed.
- [18] a) M. Di Vaira, C. A. Ghilardi, S. Midollini, L. Sacconi, *J. Am. Chem. Soc.* **1978**, *100*, 2550–2551; b) M. Caporali, L. Gonsalvi, A. Rossin, M. Peruzzini, *Chem. Rev.* **2010**, *110*, 4178–4235.
- [19] According to the integral intensities of **[5]** in comparison to those of minor products, **[5]** is formed with about 81 % conversion.
- [20] This process is reversible, as the same signals for **A** can again be observed if the probe is cooled back down.

- [21] Although the reaction pathway indicates a ratio for $\text{LiPPh}_2/\mathbf{1}$ of 1:2, the best experimental yields were achieved by using a 1:1 molar ratio. The higher ratio of LiPPh_2 probably shifts the equilibrium between **1** and **A** in favor of **A**.
- [22] M. Baudler, Y. Aktalay, K.-F. Tebbe, T. Heinlein, *Angew. Chem. Int. Ed. Engl.* **1981**, 20, 967–969; *Angew. Chem.* **1981**, 93, 1020–1022.
- [23] a) K.-O. Feldmann, J. J. Weigand, *Angew. Chem. Int. Ed.* **2012**, 51, 7545–7549; *Angew. Chem.* **2012**, 124, 7663–7667; b) M. H. Holthausen, J. J. Weigand, *Chem. Soc. Rev.* **2014**, 43, 6639–6657.
- [24] If one equivalent of LiNMe_2 is used, a wide product distribution is observed in the ^{31}P NMR spectrum and no signals can be assigned.

Received: February 19, 2016
Published online: April 21, 2016